Triply Periodic Minimal Surfaces (TPMS) for the Generation of Porous Architectures Using Stereolithography

Sébastien Blanquer, D.W. Grijpma

Triply Periodic Minimal Surfaces (TPMS) for the Generation of Porous Architectures Using Stereolithography

Sebastien B. G. Blanquer and Dirk W. Grijpma

Abstract

A new generation of sophisticated tissue engineering scaffolds are developed using the periodicity of trigonometric equations to generate triply periodic minimal surfaces (TPMS). TPMS architectures display minimal surface energy that induce typical pore features and surface curvatures. Here we described a series of TPMS geometries and developed a procedure to build such scaffolds by stereolithography using biocompatible and biodegradable photosensitive resins.

Key words Triply periodic minimal surfaces (TPMS), Minimal surface energy, Trigonometric equations, Stereolithography, Scaffold, Biodegradable polymer, Photosensitive resins

1 Introduction

Scaffold design and pore geometries play a major role in cell and tissue organization in tissue-engineered constructs. It is becoming clear that the high biological and functional complexity of the human tissues with specific (micro)architecture and vascular networks may require more specific and sophisticated scaffold geometries using appropriate multifunctional materials. The expansion of additive manufacturing technologies in the development of sophisticated scaffolds remains in constant evolution. Among the existing additive manufacturing techniques, stereolithography (SL) is recognized for its remarkable efficiency and considerable advantages in terms of versatility in manufacturing, high accuracy, and quickness. It offers unique ways to precisely control substrate architecture [1, 2]. The principle of the fabrication is based on a spatially controlled solidification by photopolymerization of monomer or prepolymer resins, in liquid or viscous state, using a single-photon source. In order to build the desired 3D structures in a layer-by-layer manner with SL, it is necessary to initially design the 3D object from a “3D computer-assisted design” (CAD) file.

In order to increase the diversity of structure and the complexity of internal porous architecture, a new approach of CAD file conception can be used. In this optic, we developed a new generation of sophisticated, stable, and highly interconnected porous scaffolds based on triply periodic minimal surfaces (TPMS) (Fig. 1) [3]. TPMS architectures are infinite and periodic in the 3D Euclidean space and belong to the interesting class of minimal surfaces [4–6]. Minimal surfaces are frequently encountered in nature and play an essential role in guiding chemical, biochemical, and cellular processes [7–10]. The natural organization of minimal surface structures responds to physical principle that governs the forms and the motions of objects, the principle of free energy minimization. In nature and man-made environments, the systems normally try to arrange themselves to minimize their potential energy in order to consume less energy and leading to a better stability [11]. Consequently, the term "minimal surface" is directly linked to the surface energy and represents the lowest possible potential energy that a surface can have if its energy is proportional to the surface area. In addition, the minimization of the surface energy leads automatically to typical curved structure with respect of the initial fixed boundary [6, 12, 13].

The study of TPMS architecture scaffolds allows to give a new dimension and vision of the tissue engineering scaffold designs. Indeed, in addition to the great benefit of such structures in terms of interconnectivity, high specific tortuosity and maximization of the specific surface area, TPMS architectures based on such concept of minimal surface energy display specific surface curvature distribution, which has been proved to be also a significant parameter that can influence cell behavior and therefore tissue formation [14, 15].

SL technique is chosen to produce these complex scaffolds using two different materials, a rubber-like material poly(trimethylene carbonate) (PTMC) and a stiff material poly(D,L-lactide) (PDLLA). The synthesis of the photosensitive resins is conveniently prepared in two successive steps with high yields (Fig. 2), and the resin was successfully used by SL to develop a library of different TPMS architecture scaffolds.

2 Materials

The described protocol requires access to a chemistry wet lab with standard equipment.

1. Trimethylene carbonate (TMC). Monomers must be stored at —20 °C in sealed containers.
2. DL-Lactide (DLLA). Monomers must be stored at —20 °C in sealed containers.

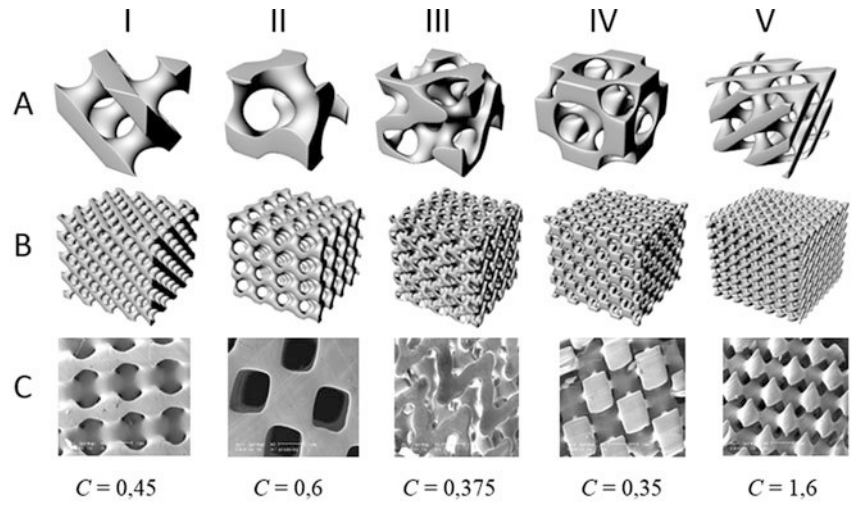

I/ $\sin(x).\sin(y).\sin(z) + \sin(x).\cos(y).\cos(z) + \cos(x).\sin(y).\cos(z) + \cos(x).\cos(y).\sin(z) = C$

II/ $\cos(x).\sin(y) + \cos(y).\sin(z) + \cos(z).\sin(x) = C$

III/ $\cos(2x).\sin(y).\cos(z) + \cos(2y).\sin(z).\cos(x) + \cos(2z).\sin(x).\cos(y) = C$

IV/ $8.\cos(x).\cos(y).\cos(z) + 1.(\cos(2x).\cos(2y).\cos(2z)) - 1.(\cos(2x).\cos(2y) + \cos(2y).\cos(2z) + \cos(2z).\cos(2.x)) = C$

V/ $1.(\sin(2x).\sin(2y) + \sin(2y).\sin(2z) + \sin(2x).\sin(2z)) + 1.(\cos(2x).\cos(2y).\cos(2z)) = C$

Fig. 1 Visualization of five TPMS scaffolds with their respective harmonic trigonometric functions. (a) CAD designs representing the repeated unit cells, (b) assemblies of 4 × 4 × 4 unit cells to create a sophisticated 3D porous structure, (c) SEM images of the built structures prepared from the PTMC resin by SL. Offset values C are chosen for each structure to reach 65% of porosity

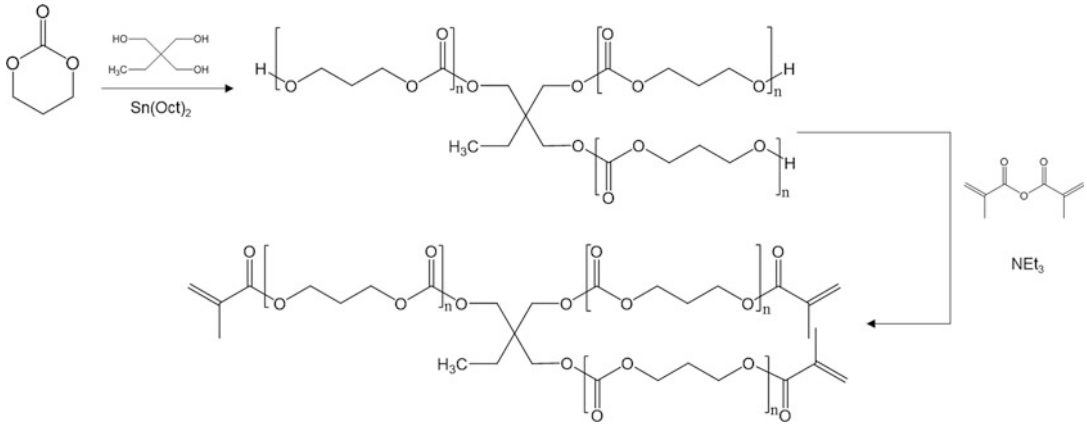

Fig. 2 Synthesis of PTMC photosensitive resin by successive ROP and end-functionalization

3. Tin 2-ethylhexanoate 92.5–100.0% (SnOct2).
4. Trimethylolpropane ≥98.0% (TMP).
5. Trimethylamine ≥99% (NEt3).
6. Methacrylic anhydride 94% (contains 2000 ppm Topanol A as inhibitor).
7. Methanol absolute.

8. Anhydrous dichloromethane ≥99%.
9. Propylene carbonate.
10. Lucirin TPO-L (ethyl 2,4,6-trimethylbenzoylphenyl phosphinate, BASF) photoinitiator.
11. Orasol Orange G (Ciba Specialty Chemicals) to control the degree of penetration of blue light in the resin.
12. Three-necked flask. Dry for several hours in an oven at 100 °C prior to use.
13. Crosslinking cabinet (Ultralum).
14. Stereolithographic 3D printer (Perfactory Mini Multilens, EnvisionTec).

3 Methods

3.1 Synthesis of the Biodegradable and Biocompatible Three-Armed Oligomers by Ring Opening Polymerization

Two types of biocompatible and biodegradable polymeric materials are investigated to prepare the TPMS scaffolds, materials based on poly(trimethylene carbonate) (PTMC) and poly(D,L-lactide) (PDLLA). A multi-gram production of polymer resin is afforded with predetermined molecular weights. Low chain length is preferred to facilitate the end-functionalization and the crosslinking steps. The configuration of the polymer (single arm, star-shaped, etc.) is determined by the initiator molecule, and the molecular weight can be adjusted by varying the monomer to the initiator molar ratio. Three-armed and hydroxy-terminated oligomers targeting 5000 g/mol as global chain length are synthesized. The targeted molecular weight of 5000 g/mol corresponds to an approximate degree of polymerization of 16 trimethylene carbonate units per arm and an approximate degree of polymerization of 23 lactic acid units per arm.

All manipulations must be performed in a fume hood. The experimenter must wear a lab coat and gloves during all the different chemical steps.

1. To synthesize three-armed PTMC, add TMC monomer (0.98 mol; 100 g), $Sn(Oct)_2$ catalyst (0.05 wt% of monomer), and TMP initiator (0.0196 mol; 2.62 g) (*see* Note 1). Add the compounds under argon into the dried flask, and apply to the mixture 10 cycles of vacuum and argon backfill at room temperature and under stirring (*see* Note 2).
2. Perform bulk polymerization for 48 h in argon atmosphere at 130 °C by heating with an oil bath.
3. Same protocol can be adjusted for the synthesis of poly(D,L-lactide) oligomers. Three-armed PDLLA oligomer synthesis is performed by ring opening polymerization of D,L-lactide (0.694 mol; 100 g), catalyzed by $Sn(Oct)_2$ (0.05 wt% of

monomer), and initiated by TMP (6.94 mmol; 0.93 g) at 130 °C for 48 h under an argon atmosphere.

4. The monomer conversion and the degree of polymerization can be determined by ^{1}H-NMR spectroscopy using $CDCl_3$ as a solvent. Assuming that each hydroxyl group of the glycerol initiates polymerization of TMC, the degree of polymerization is determined by comparing the peak integral that characterizes the -CH_2- groups of the TMC at 4.2 ppm (4H) or 2.05 ppm (2H) with the CH_3- groups from the TMP initiator at 0.8 ppm (3H). Monomer conversion is calculated from the peak integral of the PTMC at 4.2 ppm (4H) or 2.05 ppm (2H) compared to the peak integral of the TMC monomer at 4.4 ppm (4H) or 2.2 ppm (2H).
5. Same characterization and efficacy are obtained with PDLLA oligomers. The conversion is determined by the characteristic peak integral of lactide monomers at 5.05 ppm corresponding to the -CH- (1H) groups and the peak integral of the -CH- from PDLLA at 5.15 ppm. Conversion rate for both polymer types is traditionally close to 95–99%.

3.2 Preparation of the Photosensitive Resin Precursor

Following the synthesis of the hydroxy-terminated oligomers, the next step of the resin preparation consists of the end-functionalization of the oligomers by photosensitive groups able to polymerize under light initiation. This functionalization is a key step to achieve a photocrosslinkable resin. The most straightforward approach of such functionalization is to end-cap the polymer chains through the reaction of the hydroxyl end-groups with photoreactive acrylate or methacrylate groups in order to induce radical photopolymerization [16], which leads to photosensitive macromers. Radical photopolymerization is a fast, selective, and highly effective reaction, which is a crucial requirement in SL. In conventional SL technology, the resin composition includes the photosensitive polymer resin, a photoinitiator, and if necessary an inert or reactive diluent.

1. After dissolution of the hydroxy-terminated oligomers in anhydrous dichloromethane (100 mL) (*see* Note 3), add an excess of anhydrous methacrylic anhydride (0.15 mol; 22 mL) in the presence of triethylamine (0.15 mol; 20 mL). The reaction is performed at room temperature under stirring and argon atmosphere for 3 days.
2. Purify photosensitive resin by precipitation (*see* Note 4). Dispense the resin dropwise in 500 mL of ice-cold methanol inside a beaker under vigorous stirring. Recover and vacuum-dry the precipitate. A sticky white paste should be obtained.
3. The degree of functionalization can be determined by ^{1}H-NMR analysis in $CDCl_3$. Taking into account the degree

of polymerization determined previously, the end-functionalization rate is assessed by comparing the peak integral of the PTMC at 4.2 ppm (4H) or 2.05 ppm (2H) with the grafted methacrylate with the peak integral at 6.06 ppm (1H) and 5.51 ppm (1H) corresponding to the acrylate bonds CH_2-. Purity of the macromers is also evaluated by ^{1}H-NMR with the presence of the remained non-grafted methacrylate molecules with chemical shifts at 6.09 ppm (1H) and 5.51 ppm (1H). Degree of functionalization on PDLLA macromers is assessed via the integral peak at 5.15 ppm of the -CH- (1H) groups (*see* Note 5). End-functionalization of these types of macromers is 90–95% (*see* Notes 6 and 7).

3.3 Photocrosslinking Assays Using the Synthesized Macromer Resins

Prior to any building by SL, the crosslinking ability should be assessed initially on a film. Crosslinking characterization consists in the measure of the gel content.

1. Dissolve macromers in dichloromethane (30 wt%) in order to decrease the viscosity (*see* Note 8). Add Lucirin TPO-L (5 wt% relative to the macromers) (*see* Note 9).
2. Use a mold to create films with a thickness of 500 μm, and irradiate the resin for 10 min at a wavelength of 452 nm into a crosslinking cabinet under argon flow to avoid radical polymerization quenching.
3. Gel content determination is performed by a weighing method (at least in triplicate). Vacuum-dry film and weigh it to give m_0. Rinse film in dichloromethane, and refresh solvent twice. Vacuum-dry film until a constant weight is reached (m_1). Efficient crosslinking procedure should lead to gel content above 90%. The gel content is defined as:

$$\text{Gel content } (\%) = \frac{m_0}{m} \times 100 \qquad (1)$$

3.4 Computer-Assisted Design Based on Triply Periodic Minimal Surface

As a rapid prototyping process, SL can create physical 3D objects from designs obtained by computer-aided design (CAD). Such CAD files can be basically generated by graphical computer software, but it can also be obtained from data acquired with medical imaging techniques such as magnetic resonance imaging (MRI) or computed tomography (CT). In this chapter, we describe another advanced approach to generate sophisticated 3D porous structures using the periodicity of trigonometric equations to generate triply periodic minimal surfaces (TPMS) (Fig. 1) [3, 17]. TPMS are mathematically defined and are recognized to be infinite and periodic in the 3D Euclidean space and display specific surface curvatures making them interesting porous architectures for highly controllable and homogeneous scaffold designs [3, 18]. As shown in Figs. 1 and 3a, TPMS structures are periodic in three

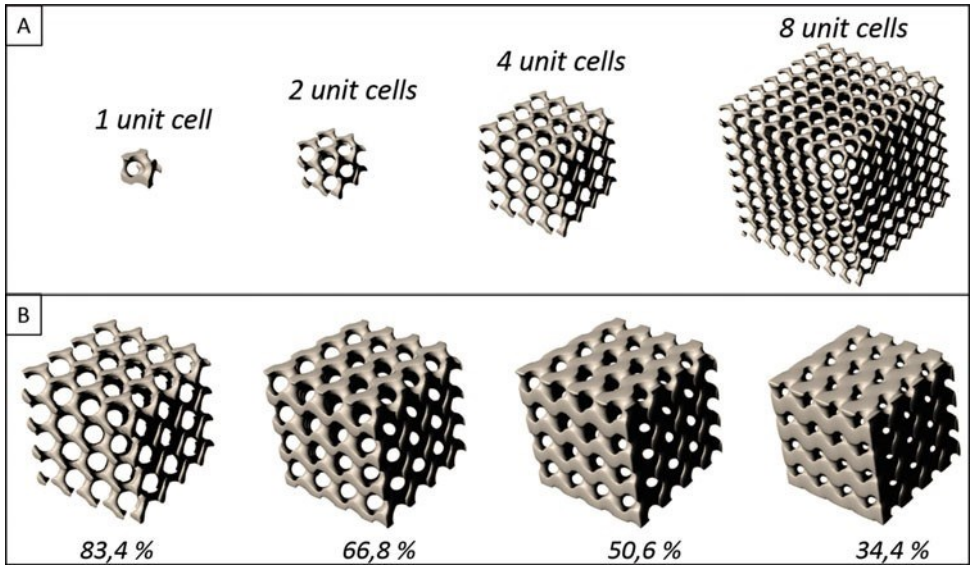

Fig. 3 Variation of the scaffolds features in terms of number of unit cells defined by the boundary conditions (a) and porosity controlled by the constant *C* (b)

independent directions and can be infinitely reproduced by repetition of cubic translational unit cells and thus can be used to construct a 3D porous scaffold.

1. Each TPMS design is defined by a trigonometric equation that is closely approximated by a periodic nodal surface [12] which leads to bicontinuous (or biphasic) TPMS porous structures. Figure 1 lists the approximated periodic nodal equations for five TPMS structures. Such approximation allows designing TPMS architectures, which therefore can form a solid/void interface where the void space represents the pores of the 3D scaffold and the solid space is materialized by the polymer.
2. TPMS designed scaffolds are obtained using K3dSurf v0.6.2 software (freeware from http://k3dsurf.sourceforge.net) that generates the CAD file. Boundary conditions must be adopted in the software to control the number of unit cells expected for the design scaffold (Fig. 3a). Consequently for scaffolds with four unit cells in x, y, and z dimensions, the boundary conditions are *x*, *y*, *z* ¼ [−4π, 4π], and a common number of 64 unit cells within the scaffold are generated. The obtained bicontinuous geometry from the TPMS structures gives a scaffold with total pore interconnectivity.
3. By modulating the linear term (*C*) to the nodal equation, it is possible to vary the pore characteristics (porosity and pore size) and the surface curvature (Fig. 3b). Therefore, the role of the constant *C* can be defined as offsetting value increasing the volume fraction of the void space. In the equations presented in

Fig. 1, the offset value has been chosen to reach 65% of porosity for all the porous structures designed and built by SL.

4. The generated CAD files can be then converted into STL files using computer-aided design software (e.g., Rhinoceros3D, McNeel). Volume scaffolds in cubic shape have been fixed to $10 \times 10 \times 10$ mm^3 for the TPMS scaffolds shown in Fig. 1.
5. EnvisionTec Perfactory RP2.0 software is used to slice the 3D CAD files in multiple layers that are sequentially fabricated by photocrosslinking.

3.5 Preparation of TPMS Scaffolds by Stereolithography

Of crucial importance in the development of precise 3D scaffold structure are not only the designed models imagined but also the types of biomaterials employed as they influence the fabrication and the properties of the fabricated 3D objects. To be used in SL, the resins should rapidly solidify upon illumination with light. In addition, SL is recognized for its high accuracy and resolution in terms of fabrication, and therefore it is necessary to develop a calibration procedure of the apparatus for each new resin batch.

1. Digital light processing (DLP) SL with a top-down approach is used to fabricate the different TPMS scaffolds. SL apparatus is equipped with a digital mirror device allowing projections of 1280×1024 pixels, each measuring 16×16 μm^2. The wavelength of the blue light irradiation ranges from 400 to 550 nm, with a peak at 440 nm.
2. For appropriate use with SL, the resin should be liquid or semi-viscous in order to ensure the transfer from liquid to a cross-linked solid. Hence, adjust resin viscosity by diluting it with a nontoxic solvent such as propylene carbonate (for both types of resin PTMC and PDLLA) in mass proportion 25 wt%.
3. In order to initiate the photopolymerization, a photoinitiator with a decomposition wavelength in adequacy with the light irradiation of the machine (*see* Note 10). Add Lucirin TPO-L photoinitiator (5 wt% relative to the macromer) and Orasol Orange dye (0.15 wt% relative to the macromer) to control the penetration depth of blue light. The resin is then dark orange (*see* Note 11).
4. Top-down approach of fabrication implies fixation of the first layer of the building to a glass support platform. The first layer is therefore solidified and attached to the platform by photocrosslinking. After photopolymerization of the first layer, the platform is moved away from the surface, and the liquid/viscous resin should then refill the space in order to allow the curing of the second layer. The layer-by-layer procedure continues until the complete fabrication of the designed structure (*see* Note 12).

5. Once the resin is prepared, the machine is calibrated through a working curve in order to precisely control the depth of cure in the resin layers. This working curve is established by measuring the photocrosslinked layer thickness for several exposure time at a certain intensity of irradiation. The correlation between the exposure time and the thickness layer expected during the building by the SL can be made using an adapted equation from the Beer-Lambert equation. This procedure has been excellently described and explained in the review from Melchels et al. [2]. On average for the PTMC and PDLLA resins, the required curing time is around 50 s with a light intensity of 18 mW/cm^2 for a sequentially layer thickness of 25 µm.
6. 3D fabrication occurs in a resin bath comprising a non-UV-absorbing plate (e.g., quartz, PDMS, etc.). For a support platform of 100 cm^2, the resin bath should have a surface of at least 120 cm^2 for a global volume of resin around 25 mL (*see* Note 13). Such volume is required to make twice building of 20 cubic scaffolds (1 cm^3).
7. After building, collect scaffolds from the platform and remove non-reacted resin by several extraction cycles (*see* Note 14). Extract non-reacted resin in 100% propylene carbonate, refreshing solvent three times a day. Exchange propylene carbonate by acetone in order to facilitate the drying step with the following acetone/propylene carbonate ratios: 20:80, 50:50; 75:25, and finally 100% acetone. Vacuum-dry scaffolds for several hours (*see* Note 15).
8. Structural and textural scaffold characterizations are performed by scanning electron microscopy (SEM) and micro-computed tomography (µCT) (*see* Note 16). Pore features in terms of interconnectivity, porosity, pore distribution, and strut thickness distribution can be assessed by these visualization analyses [3, 19].

4 Notes

1. The monomers are stored at −20 °C, and consequently before the polymerization, it is advised to equilibrate the monomers batches at room temperature before opening the sealed container.
2. Ring opening polymerization must be done in rigorous anhydrous environment. The presence of water initiates the ring opening polymerization.
3. Solubilization of PTMC or PDLLA oligomers is facilitated by stirring, but even then, it may require some time for high amounts of material.

4. All the final compounds included in the scaffolds are suited for biomedical applications. Intermediary reagents and by-products are removed during the procedure of purification for each step of the synthesis.
5. Ungrafted methacrylates from methacrylate anhydride or methacrylic acid are visible in the NMR spectra at different chemical shifts than the methacrylates grafted to the polymer, which therefore allows the reaction process to be followed, and the elimination of unreacted methacrylates by precipitation.
6. The methacrylated polymers can be defined as a photoactive resin, macromer, macromonomer, or prepolymer.

   In the absence of photoinitiator, the acrylate groups are hardly susceptible to photo-curing; however it is recommended to protect the resin from light during storage and building process to prevent premature crosslinking. It is recommended to store resin batches in a freezer, especially for PDLLA resins, which are highly sensible to degradation by hydrolysis.
7. Drying procedures must be performed under vacuum at room temperature. Rising the temperature may initiate unexpected thermal crosslinking.
8. Optimal viscosity has been found around 10 Pa·s; however higher or lower viscosity can also be used. Viscosity can be adjusted by dilution in a solvent with high boiling temperature to prevent evaporation and modification of the resin concentration. Use of an apparatus equipped with heater can also be suggested to reduce the viscosity.
9. The end-functionalization reaction might lead to a yellow solution, which is due to the oxidation of the trimethylamine added in the reaction but does not impair the efficiency of the reaction.
10. Radical photopolymerization of methacrylates is known to be efficient and fast, but in case of low crosslinking efficiency or weak mechanical properties of the building object, curing can be enhanced using a reactive solvent (e.g., NVP) or crosslinker (e.g., di- or tri-acrylate).
11. Dyes such as Orange Orasol are suggested in order to avoid the over-curing of the resin into a preceding layer.
12. Radical photopolymerization is inhibited in presence of oxygen, and the reaction should be ideally maintained continuously under flow of inert gas like argon or nitrogen. This caution can be taken conveniently during the initial curing tests process using a UV cabinet but remains hard to set up during the building by SL. That is why the bottom-up approach significantly limits the contact with the environment and the photopolymerization is only little impaired by oxygen.

13. Volume of the resin may be adjusted to fit the size of the support platform.
14. Solvent extraction is a critical step as the swelling effect may damage or destroy the scaffolds. Consequently, acetone can be substituted by ethanol. Nevertheless, purification of the scaffolds by solvent extraction must be done carefully and necessarily sequentially. Supernatant from the extraction steps should be intensely orange-colored for the first steps and completely clear for the last steps.
15. In this process, the conversion of reactive groups is usually incomplete, and post-thermal curing (90 °C for 5 h) is often applied to convert unreacted methacrylate functions into the polymer network.
16. Due to the formation of a chemical network during the building by SL, the solvent is present in the network, and therefore the size of the 3D object changes upon drying. The sizes of the designs should be adjusted to the diluent concentration in order to give scaffolds with desired sizes after building, extracting, and drying.

References

1. Bartolo PJ (2011) Stereolithography: materials, processes and applications. Springer, New-York, NY. ISBN 978-0-387-92904-0
2. Melchels FPW, Feijen J, Grijpma DW (2010) A review on stereolithography and its applications in biomedical engineering. Biomaterials 31(24):6121–6130
3. Blanquer SBG, Werner M, Hannula M, Sharifi S, Lajoinie GPR, Eglin D, Hyttinen J, Poot AA, Grijpma DW (2017) Surface curvature in triply-periodic minimal surface architectures as a distinct design parameter in preparing advanced tissue engineering scaffolds. Biofabrication 9(2):025001
4. Fischer W, Koch E (1987) On 3-periodic minimal-surfaces. Z Kristallogr 179(1–4):31–52
5. Schoen AH (2012) Reflections concerning triply-periodic minimal surfaces. Interface Focus 2(5):658–668
6. Hyde S, Andersson S, Larsson Z, Blum T, Landh S, Lidin BW, Ninham BW (1997) The language of shape: the role of curvature in condensed matter: physics, chemistry and biology. Elsevier, Amsterdam
7. Mai YY, Eisenberg A (2012) Self-assembly of block copolymers. Chem Soc Rev 41 (18):5969–5985
8. Angelova A, Angelov B, Mutafchieva R, Lesieur S, Couvreur P (2011) Self-assembled multicompartment liquid crystalline lipid carriers for protein, peptide, and nucleic acid drug delivery. Acc Chem Res 44(2):147–156
9. Tenchov B, Koynova R (2012) Cubic phases in membrane lipids. Eur Biophys J Biophys 41 (10):841–850
10. Urbas AM, Maldovan M, DeRege P, Thomas EL (2002) Bicontinuous cubic block copolymer photonic crystals. Adv Mater 14 (24):1850–1853
11. Eriksson JC, Ljunggren S (1994) The mechanical surface-tension and stability of minimal surface-structures. J Colloid Interface Sci 167 (2):227–231
12. Gandy PJF, Bardhan S, Mackay AL, Klinowski J (2001) Nodal surface approximations to the P, G, D and I-WP triply periodic minimal surfaces. Chem Phys Lett 336(3–4):187–195
13. Mackay AL (1994) Periodic minimal-surfaces from finite-element methods. Chem Phys Lett 221(3–4):317–321
14. Rumpler M, Woesz A, Dunlop JWC, van Dongen JT, Fratzl P (2008) The effect of geometry on three-dimensional tissue growth. J R Soc Interface 5(27):1173–1180
15. Werner M, Blanquer SBG, Haimi SP, Korus G, Dunlop JWC, Duda GN, Grijpma DW, Petersen A (2017) Surface curvature differentially regulates stem cell migration and

differentiation via altered attachment morphology and nuclear deformation. Adv Sci 4 (2):1600347

16. Matsuda T, Mizutani M (2002) Liquid acrylate-endcapped biodegradable poly(epsilon-caprolactone-co-trimethylene carbonate). II. Computer-aided stereolithographic microarchitectural surface photoconstructs. J Biomed Mater Res 62(3):395–403
17. Schoen AH (1970) Infinite periodic minimal surfaces without self-intersections. NASA Technical report TN D-5541, Washington, DC
18. Yoo DJ (2011) Porous scaffold design using the distance field and triply periodic minimal surface models. Biomaterials 32 (31):7741–7754
19. Narra N, Blanquer SBG, Haimi SP, Grijpma DW, Hyttinen J (2015) mu CT based assessment of mechanical deformation of designed PTMC scaffolds. Clin Hemorheol Microcirc 60(1):99–108